Mechanistic Studies of Si−CN and C−NC Bond Activation of Silylnitriles and Alkyl Isonitriles by Rhodium Porphyrin Radical: Novel Cyanide Transfer

Lirong Zhang, Chun Wah Fung, and Kin Shing Chan*

Department of Chemistry, The Chinese University of Hong Kong, Shatin, New Territories, Hong Kong, People's Republic of China

Received June 16, 2006

The Si−CN and C−NC bonds of silylnitriles and alkyl isonitriles were activated by (tetramesitylporphyrinato)rhodium(II), Rh(tmp), to give rhodium porphyrin silyls or alkyls and rhodium porphyrin cyanide, respectively. Pyridine and triphenylphosphine promoted the rates and yields of the reactions with silylnitriles, but inhibited the rates and yields of the reactions with isonitriles. The reaction of Rh(tmp) with Me_3SiCN exhibited second-order kinetics (rate = k_{obs}[Rh(tmp)][Me_3SiCN]) at a sufficiently high concentration of pyridine. The reaction with BuNC showed fourth-order kinetics, second-order in each of the reactants; rate = k_{obs}[Rh(tmp)]^2[BuNC]^2. A novel cyanide transfer rate-determining step was proposed to account for the reaction mechanism.

Introduction

Rhodium(II) tetramesitylporphyrin, Rh(tmp) (Figure 1), is a metalloradical and exhibits rich chemistry. Wayland and others have reported extensively on the bond activation and spectroscopy of Rh(tmp) metalloradical. Some typical bond activations by Rh(tmp) include activation of the carbon−hydrogen bond of hydrocarbon H−CH_2R,[1,2] abstraction of the allylic hydrogen atom from methyl methacrylate,[3] halogen atom abstraction from a wide variety of organic halides,[4] and activation of carbon−isonitrile bonds.[5] Rh^{II}(por) (por = oep (octaethylporphyrin), tpp (tetraphenylporphyrin), tmp) also react with H_2/CO mixtures to yield rhodium formyl derivatives.[6] The metal−metal bonded dimers of Rh(II) porphyrins also exhibit wide activities, such as carbon−hydrogen bond activation and abstraction of a hydrogen atom.[7,8]

Rh(tmp) exhibits unique coordination chemistry. The coordination complexes Rh(tmp)L (L = NEt_3, $NHEt_2$, py, 2,6-Me_2-py, PEt_3, PPh_3, $AsPh_3$, CNR) have been stabilized at 90 K in toluene or methyl cyclohexane and have been characterized by ESR.[9,10] Some of the complexes are unstable. Wayland has suggested that the disproportionation of certain Rh^{II}(por) to Rh^{I}(por) and Rh^{III}(por) is driven by the favorable thermodynamics associated with binding an axial ligand to the Rh(III) product to account for the instability.[11,12] A rhodium to porphyrin electron transfer mechanism has also been proposed by Collman.[10]

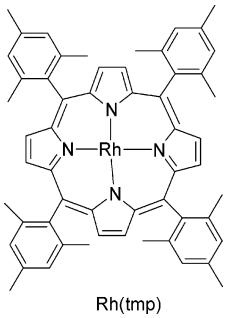

Rh(tmp)

Figure 1. Structure of Rh(tmp).

In our continuing interest in the rich chemistry of rhodium porphyrins in bond activations, we have recently reported that Rh(tmp)[2a] activates unstrained aliphatic carbon−carbon bonds of nitroxides to yield rhodium porphyrin alkyls.[13,14] Expanding the scope of substrates, we have found that Rh(tmp) undergoes a formal silicon−nitrogen bond activation[15] with silylnitriles.[16−18]

* Corresponding author. E-mail: ksc@cuhk.edu.hk.

(1) Sherry, A. E.; Wayland, B. B. *J. Am. Chem. Soc.* **1990**, *112*, 1259−1261.

(2) (a) Wayland, B. B.; Ba, S.; Sherry, A. E. *J. Am. Chem. Soc.* **1991**, *113*, 5305−5311. (b) Del Rossi, K. J.; Zhang, X. X.; Wayland, B. B. *J. Organomet. Chem.* **1995**, *504*, 47−56. (c) Del, Rossi, K. J.; Wayland, B. B. *J. Chem. Soc., Chem. Commun.* **1986**, 1653−1655.

(3) Wayland, B. B.; Poszmik, G.; Fryd, M. *Organometallics* **1992**, *11*, 3534−3542.

(4) Anderson, J. E.; Yao, C.-L.; Kadish, K. M. *Inorg. Chem.* **1986**, *25*, 718−719.

(5) Poszmik, G.; Carroll, P. J.; Wayland, B. B. *Organometallics* **1993**, *12*, 3410−3417.

(6) (a) Farnos, M. D.; Woods, B. A.; Wayland, B. B. *J. Am. Chem. Soc.* **1986**, *108*, 3659−3663. (b) Wayland, B. B.; Van Voorhees, S. L.; Wilker, C. *Inorg. Chem.* **1986**, *25*, 4039−4024. (c) Van Voorhees, S. L.; Wayland, B. B. *Organometallics* **1985**, *4*, 1887−1888.

(7) Farnos, M. D.; Woods, B. A.; Wayland, B. B. *J. Am. Chem. Soc.* **1986**, *108*, 3659−3663.

(8) (a) Jones, W. D.; Feher, F. J. *Acc. Chem. Res.* **1989**, *22*, 2, 91−100. (b) Selmeczy, A. D.; Jones, W. D.; Osman, R.; Perutz, R. N. *Organometallics* **1995**, *14*, 5677−5685.

(9) Wayland, B. B.; Sherry, A. E. Bunn, A. G. *J. Am. Chem. Soc.* **1993**, *115*, 7675−7684.

(10) Collman, J. P.; Boulvtov, R. *J. Am. Chem. Soc.* **2000**, *122*, 11812−11821.

(11) Ni, Y.; Fitzgerald, J. P.; Carroll, P.; Wayland, B. B. *Inorg. Chem.* **1994**, *33*, 2029−2035.

(12) Wayland, B. B.; Balkus, K. J., Jr.; Farnos, M. D. *Organometallics* **1989**, *8*, 950−955.

(13) Tse, M. K.; Chan, K. S. *Dalton* **2001**, 510−511.

(14) Mak, K. W.; Yeung, S. K.; Chan, K. S. *Organometallics* **2002**, *21*, 2362−2364.

(15) Sakkai, S.; Ieki, M. *J. Am. Chem. Soc.* **1993**, *115*, 2373−2381.

(16) (a) Churchill, D.; Shin, J. H.; Hascall, T.; Hahn, J. M.; Bridgewater, B. M.; Parkin, G. *Organometallics* **1999**, *18*, 2403−2406. (b) Taw, F. L.; White, P. S.; Bergman, R. G.; Brookhart, M. *J. Am. Chem. Soc.* **2002**, *124*, 4192−4193.

10.1021/om0605276 CCC: $33.50
Publication on Web 09/22/2006

Table 1. Reaction of Silylnitriles with Rh(tmp)

entry	substrate[a]	ligand	temp/°C	time	product (% yield)[d]	
1	Me_3SiCN	none	110	8 h	Rh(tmp)$SiMe_3$ (16)	Rh(tmp)CN (14)
2	Me_3SiCN	py[b]	70	3 h	Rh(tmp)$SiMe_3$ (71)	pyRh(tmp)CN (72)
3	Me_3SiCN	py[b]	90	1 h	Rh(tmp)$SiMe_3$ (73)	pyRh(tmp)CN (70)
4	Me_3SiCN	py[b]	110	1 h	Rh(tmp)$SiMe_3$ (88)	pyRh(tmp)CN (81)
5	Me_3SiCN	py[b]	130	1 h	Rh(tmp)$SiMe_3$ (82)	pyRh(tmp)CN (84)
6	Me_3SiCN	Ph_3P[c]	110	3 h	Rh(tmp)$SiMe_3$ (79)	Rh(tmp)CN (78)
7	$^tBuMe_2SiCN$	py[b]	110	1 d	Rh(tmp)Si^tBuMe_2 (18)	pyRh(tmp)CN (85)
8	$^tBuMe_2SiCN$	py[b]	130	1 d	Rh(tmp)Si^tBuMe_2 (22)	pyRh(tmp)CN (80)
9	$^tBuMe_2SiCN$	Ph_3P[b]	110	1 d	Rh(tmp)Si^tBuMe_2 (2)	

[a] 10 equiv of silyl cyanide. [b] 2 equiv of pyridine. [c] 1 equiv of Ph_3P. [d] Isolated yield.

Mechanistic studies of the reaction of Me_3SiCN reveal a novel cyanide group transfer as the key mechanistic step in the bond activation.[18] In examining the generality of the cyanide transfer process, we have carried out further mechanistic studies of the activation of alkyl isonitriles with Rh(tmp) and now disclose the full results.

Results and Discussion

Reactions with Me_3SiCN. Initially, when the reaction of ^{t}BuCN with Rh(tmp) in benzene was examined, no reaction was observed at 70 °C in 5 days. We reasoned that silylnitriles might be more reactive substrates since they are sterically less hindered with longer Si−CN bond lengths (Me_3SiCN: 1.84 Å;[19] BDE_{Si-CN} = 85 kcal mol^{-1})[20] than C−CN bonds (CH_3CN: 1.46 Å;[21] BDE_{Me-CN} = 117 kcal mol^{-1}).[22] To our delight, a solution of Rh(tmp)[2a,13] in benzene reacted with 10 equiv of Me_3SiCN at 110 °C for 8 h to give Rh(tmp)$SiMe_3$[23] and Rh(tmp)CN[3] in 16% and 14% yield, respectively (eq 1; Table 1, entry 1). The silicon−CN bond was activated, but the yields were rather poor. Encouraged by this successful formal Si−CN activation, we sought to optimize the yields.

$$2\mathrm{Rh(tmp)} + \mathrm{RMe_2SiCN} \xrightarrow[\mathrm{C_6H_6,\ N_2}]{\text{ligand}} \mathrm{Rh(tmp)SiRMe_2} + \mathrm{LRh(tmp)CN} \quad (1)$$

Ligands are known to enhance the reactivity of Rh(por).[9,10] Indeed, when pyridine was added, both the rates and yields of reaction were increased, with Rh(tmp)$SiMe_3$ and *trans*-pyRh(tmp)CN isolated in 88% and 81% yields, respectively (Table 1, entries 2−5). Rh(tmp)$SiMe_3$ did not show any change of proton chemical shift in benzene-d_6 with excess pyridine added. Rh(tmp)$SiMe_3$, therefore, did not coordinate with pyridine either in solution or in the solid state after isolation, presumably due to the strong trans effect of the silyl group. The rates of reactions and yields of the products increased slightly from 70 to 130 °C (Table 1, entries 2−5).

When triphenylphosphine was used, the rate and yield were enhanced. However, compared with the reaction with pyridine added, a longer reaction time of 3 h was required with little change of product yields (Table 1, entry 6). Rh(tmp)CN was also obtained without any Ph_3P coordinated, and it dissolved poorly in solvent, making isolation difficult. Pyridine is therefore a more effective ligand promoter.

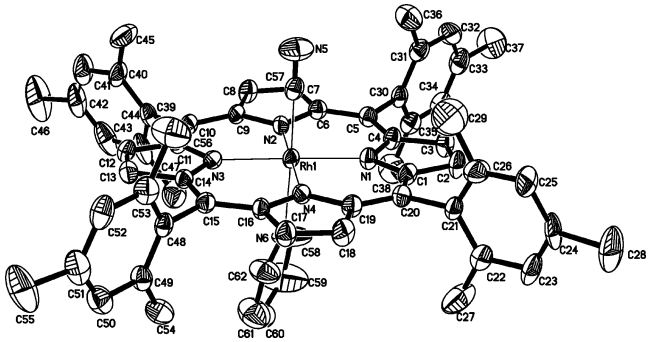

Figure 2. Molecular structure of pyRh(tmp)CN, showing the atomic labeling scheme and 30% probability displacement ellipsoids.

Reactions of ^{t}BuMe$_2$SiCN. When the sterically more hindered ^{t}BuMe$_2$SiCN was reacted with Rh(tmp), silicon−nitrile bond activation occurred at 130 °C in the presence of added pyridine. A lower yield of Rh(tmp)Si^tBuMe_2 of 22% was observed, while pyRh(tmp)CN was still obtained in a high yield of 80% (Table 1, entries 7 and 8). Reaction at 110 °C gave similar reaction rates and product yields. When triphenylphosphine was used, only a small amount of Rh(tmp)Si^tBuMe_2 was produced (Table 1, entry 9). To understand why the yield of Rh(tmp)Si^tBuMe_2 was so low, the thermal stability of Rh(tmp)Si^tBuMe_2 was examined. Since Rh(tmp)Si^tBuMe_2 in benzene with or without excess pyridine or triphenylphosphine added was thermally stable at 110 °C for at least 1 day, the poor yield of Rh(tmp)Si^tBuMe_2 is ascribed to the higher kinetic barrier in its formation presumably due to steric hindrance.

X-ray Structure of pyRh(tmp)CN. pyRh(tmp)CN was characterized by single-crystal X-ray analysis. The structure shows that pyridine is trans to the cyanide group. The angles of N(3)−Rh−N(1) and N(4)−Rh−N(2) are 178.9° and 179.8°, respectively (Figure 2). Also the distances of Rh with four nitrogen atoms in the pyrroles are nearly the same at 2.036 Å. Therefore, the Rh is in the center of the pyrrolic nitrogen ring. The bond length between the metal Rh and cyanide group is 1.983 Å, which is shorter than the bond length of Rh and pyridine (2.157 Å). The cyanide group and pyridine ligand are in an almost linear form (N(6)−Rh(1)−C(7) = 178 (4)°).

The porphyrin ring is a plane with a small twist. The Rh atom is displaced 0.025 Å from the porphyrin-core atom defined by the corresponding 24-atom least-squares plane toward pyridine. The largest deviation relative to the mean plane of the pyrrole ring is at C_{20} (0.1194 Å), whereas N_3 lies approximately above the mean plane by about 0.0703 Å. The dihedral angles between mesitylphenyl plane and the mean

(17) (a) Edelbach, B. L.; Lachicotte, R. J.; Jones, W. D. *Organometallics* **1999**, *18*, 4660−4668. (b) Huang, D.; Heyn, R. H.; Bollinger, J. C.; Caulton, K. G. *Organometallics* **1997**, *16*, 292−293.

(18) Chan, K. S.; Zhang, L.; Fung, C. W. *Organometallics* **2004**, *23*, 6097−6098.

(19) Zanchini, C. *Chem. Phys.* **2000**, *254*, 187−202.

(20) Corey. J. Y. In *The Chemistry of Organic Silicon Compounds Part 1*; Patai, S., Rappoport, Z., Ed.; John Wiley & Sons Ltd.: New York, 1989; pp 5−6.

(21) *Tables of Interatomic Distances and Configuration in Molecules and Ions*; The Chemical Society: London, 1958.

(22) Luo, Y.-R. *Handbook of Bond Dissociation Energies in Organic Compounds*; CRC Press: Boca Raton, FL, 2003.

(23) Tse, A. K.-S.; Wu, B.-M.; Mak, T. C. W.; Chan, K. S. *J. Organomet. Chem.* **1998**, *568*, 257−261.

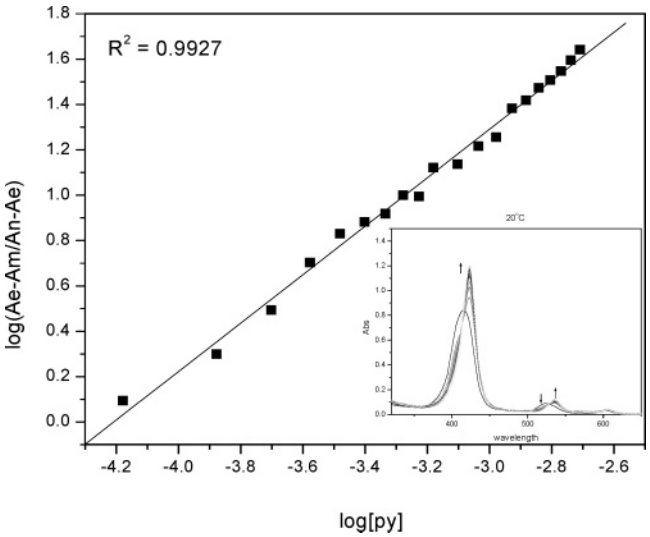

Figure 3. UV titration and analysis curves of Rh(tmp) with pyridine at 20 °C.

porphyrin plane are 78.1°, 86.2°, 87.8°, and 81.8°, respectively. The dihedral angles between NC_4 pyrroles and the mean plane are 2.9°, 1.3°, 0.6°, and 3.3°, respectively.

UV Titration of [Rh(tmp)] and Pyridine. The stoichiometry and binding constants of Rh(tmp) and pyridine were measured spectrophotometrically at 536 nm from 20 to 40 °C (eq 2). The titration curves of Rh(tmp) with pyridine at 20.0 °C are shown in Figure 3. Analyses of the data confirmed a 1:1 adduct and yielded the binding constants at 30.0 °C: K_1 ($= k_1/k_{-1} = 1.87 \times 10^4 \pm 1.10$ M^{-1}). The enthalpy and entropy of the pyridine coordination were estimated, by plotting ln K_1 against $1/T$ (Figure 4), to be $\Delta H_1 = -10 \pm 1$ kcal mol^{-1} and $\Delta S_1 = -12 \pm 2$ cal mol^{-1} K^{-1}, respectively. The negative entropy was due to the loss of rotational and translational freedom of the ligand and the rhodium porphyrin upon coordination.

$$\mathrm{Rh(tmp)} + \mathrm{py} \underset{k_{-1}}{\overset{k_1}{\rightleftharpoons}} \mathrm{pyRh(tmp)} \quad (2)$$

Table 2 shows the results of the rates (k_1) measured from 25 to 70 °C and demonstrated that the rates were fast.

Mechanistic Studies of the Reaction of Rh(tmp) and Me_3SiCN with Pyridine in Benzene. The reaction between Rh(tmp) and Me_3SiCN with added pyridine was clean and high-yielding. Therefore, kinetic studies were carried out to evaluate the reaction orders, rate constants, and activation parameters for mechanistic understandings.

$$2\mathrm{Rh(tmp)} + \mathrm{py} + \mathrm{Me_3SiCN} \rightarrow \mathrm{Rh(tmp)SiMe_3} + \text{py-Rh(tmp)CN} \quad (3)$$

Kinetic studies of reaction 3 were performed spectrally at 538 nm under the following conditions: 70.0 °C, initial concentrations (3.28−9.06) × 10^{-5} M Rh(tmp), (0.61−6.21) × 10^{-2} M Me_3SiCN, and (0.01−4.80) × 10^{-3} M pyridine. All reactions were monitored for at least 4 half-lives and yielded straight lines of pseudo-first-order kinetic plots (Figure 5). Therefore the reaction is first-order in [Rh(tmp)]. Values of k'_{obs} were derived from the slopes of such plots. Kinetic measurements yielded the rate law shown in eq 4. The initial [Rh(tmp)] concentration was varied over at least a 3-fold range to establish the independence of k'_{obs} from [Rh(tmp)] (Table 3, entries 2 and 3). Under the conditions of the measurements with Me_3SiCN always in at least 10-fold excess over Rh(tmp), the

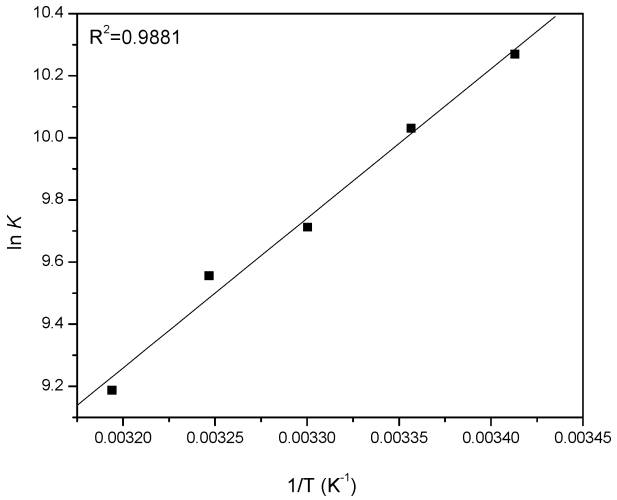

Figure 4. van't Hoff plot of the binding of Rh(tmp) with pyridine.

observed kinetics were pseudo-first-order, in accord with eq 5. Pseudo-first-order rate constants k'_{obs} were plotted against the concentration of Me_3SiCN to yield linear plots, with a typical one shown in Figure 6. The rates were also measured from 60 to 90 °C. The rate constants k_{obs}, derived from the slopes of these plots, are summarized in Table 3.

$$\text{Rate} = k'_{obs}[\mathrm{Rh(tmp)}]_0[\mathrm{Me_3SiCN}] \quad (4)$$

$$= k_{obs}[\mathrm{Rh(tmp)}]_0 \quad (5)$$

Proposed mechanism:

$$\mathrm{Rh(tmp)} + \mathrm{py} \underset{k_{-1}}{\overset{k_1}{\rightleftharpoons}} \mathrm{pyRh(tmp)} \quad (6)$$

$$\mathrm{pyRh(tmp)} + \mathrm{Me_3SiCN} \underset{k_{-2}}{\overset{k_2\ (\mathrm{rds})}{\rightleftharpoons}} \mathrm{pyRh(tmp)CN} + \mathrm{SiMe_3} \quad (7)$$

$$\mathrm{pyRh(tmp)} + \mathrm{SiMe_3} \xrightarrow{k_3} \mathrm{Rh(tmp)SiMe_3} + \mathrm{py} \quad (8)$$

$$\text{Rate} = \mathrm{d[Rh(tmp)]}/2\mathrm{d}t = \mathrm{d[Rh(tmp)SiMe_3]}/\mathrm{d}t = k_3[\mathrm{pyRh(tmp)}][\mathrm{SiMe_3}] \quad (9)$$

$$\mathrm{d[SiMe_3]}/\mathrm{d}t = 0 \text{ (under steady-state conditions)} \quad (10)$$

$$k_2[\mathrm{pyRh(tmp)}][\mathrm{Me_3SiCN}] = k_{-2}[\mathrm{pyRh(tmp)CN}][\mathrm{SiMe_3} + k_3[\mathrm{pyRh(tmp)}][\mathrm{SiMe_3}] \quad (11)$$

So

$$[\mathrm{SiMe_3}] = \frac{k_2[\mathrm{pyRh(tmp)}][\mathrm{Me_3SiCN}]}{k_{-2}[\mathrm{pyRh(tmp)CN}] + k_3[\mathrm{pyRh(tmp)}]} \quad (12)$$

$$\text{Rate} = \frac{k_3k_2[\mathrm{pyRh(tmp)}]^2[\mathrm{Me_3SiCN}]}{k_{-2}[\mathrm{pyRh(tmp)CN}] + k_3[\mathrm{pyRh(tmp)}]} \quad (13)$$

When

$$k_3[\mathrm{pyRh(tmp)}] \gg k_{-2}[\mathrm{pyRh(tmp)CN}] \quad (14)$$

$$\text{Rate} = \frac{K_1[\mathrm{py}][\mathrm{Rh(tmp)}]_0}{1 + K_1[\mathrm{py}]}k_2[\mathrm{Me_3SiCN}] \quad (15)$$

At high [py] so that K_1[py] ≫1, rate is independent of [py].

Table 2. Rate Constants of Reaction 2

entry	temp/°C	[Rh(tmp)] × 10^5/M	[py] × 10^3/M	$k'_{obs\ (2)} \times 10/s^{-1}$	$k_{obs} \times 10^{-1}/M^{-1}\ s^{-1}$
1	25.0	9.61	1.03	0.19 ± 0.002	1.85 ± 0.02
2	45.0	9.61	1.03	0.28 ± 0.007	2.72 ± 0.07
3	60.0	9.61	1.03	0.59 ± 0.011	5.73 ± 0.11
4	70.0	9.61	1.03	1.08 ± 0.018	10.49 ± 0.18

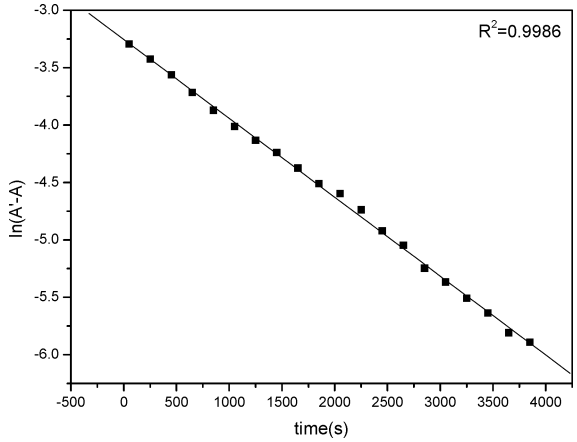

Figure 5. Pseudo-first-order rate plot for reaction 3.

The rate was independent of pyridine at sufficiently high concentration ($\geq 5.0 \times 10^{-4}$ M) and exhibited saturation kinetics in pyridine (see Figure S1, Table S1). The rate of pyridine coordination (k_1) was measured to be faster than the bond activation.

All the above results are most readily accommodated by the proposed mechanism depicted in eqs 6−8, with reaction 6 attaining a fast preequilibrium and the formal cyanide group transfer step to rhodium in reaction 7 being the rate-determining irreversible step.

A Me_3Si radical is also formed in steady-state concentration and reacts with pyRh(tmp) very rapidly. Therefore, the steady-state approximation of the trimethylsilyl radical was introduced. The rate law could be deduced to be eq 13.

In the presence of 10 equiv of pyRh(tmp)CN with respect to the Rh(tmp) concentration, the reaction rate did not vary within experimental error (Table 3, entries 3−5). Hence, k_{-2}[pyRh(tmp)CN] ≪ k_3[pyRh(tmp)] is justified and the backward reaction rate of step 7 is not important. The rate law was simplified as shown in eq 15.

Substitution of extrapolated values of K_1 at 60 to 90 °C from eq 6 allows the estimation of k_2 in eq 15. At high concentration of pyridine, K_1[py] is much larger than 1, so that k_{obs} is approximately equal to k_2; hence the rate law could be simplified as eq 16.

The Eyring plot of eq 16 is shown in Figure 7 for the determination of the activation parameters of reaction 3. Evaluation of the activation parameters concerning k_2 from 60 to 90 °C yielded $\Delta H_2^{\ddagger} = 13.1 \pm 1.3$ kcal mol^{-1} and $\Delta S_2^{\ddagger} = -26.3 \pm 3.7$ cal $mol^{-1}\ K^{-1}$.

Kinetic studies indicate that the reaction of Rh(tmp) and Me_3SiCN with pyridine added is bimolecular with a rate that is first-order in both Rh(tmp) and Me_3SiCN. The entropy of activation is in the range expected for a bimolecular process.[24]

The results of the kinetic studies identified the formal Si−CN bond cleavage of Me_3SiCN by rhodium(II) porphyrin radical via oxidative addition. A few plausible mechanisms exist for the formal oxidative addition of a Si−CN bond. (1) An electron transfer mechanism via disproportionation of pyRh(tmp) occurs to yield $[pyRh^{III}(tmp)]^+$ and $[pyRh^{I}(tmp)]^-$,[9,25a] which may react in an electrophilic or a nucleophilic manner, respectively, with Me_3SiCN. The pathways involving $[pyRh^{III}(tmp)]^+$ and $[pyRh^{I}(tmp)]^-$ existing in preequilibrium or being involved in the rate-controlling step are ruled out, since neither $[pyRh^{III}(tmp)]^+$ nor $[pyRh^{I}(tmp)]^-$ reacted with Me_3SiCN to yield Rh(tmp)$SiMe_3$. Therefore, the pyRh(tmp) radical is the reacting species. Another possible mechanism involves an outer-sphere electron transfer to the cyanide group from a six-coordinate Rh(II) complex in a prior association step and is depicted by eqs 17−19.[25b] However, our results are not consistent with this mechanism. This outer-sphere electron transfer would suggest the third-order rate law, k'[pyRh(tmp)][Me_3SiCN][py], expected for this mechanism and the binding of Rh(tmp) and pyridine in the ratio of 1:2. Therefore, the outer-sphere mechanism is ruled out.

$$pyRh(tmp) + py \rightleftharpoons Rh(tmp)py_2 \quad (17)$$

$$py_2Rh(tmp) + Me_3SiCN \rightarrow pyRh(tmp)CN + SiMe_3 + py \quad (18)$$

$$pyRh(tmp) + SiMe_3 \rightarrow Rh(tmp)SiMe_3 + py \quad (19)$$

(2) A classical two-electron oxidative addition process can occur with the involvement of a formal, neutral cis-silyl Rh(IV) cyanide intermediate, which then yields Rh(tmp)CN and a silyl radical. This mechanism is less preferred, as a crowded side-on cis coordination[26] of silyl cyanide to rhodium is necessary. Furthermore, this pathway requires an uncommon highly energetic and crowded seven-coordinated Rh(IV)[27] organometallic species.

(3) A one-electron oxidative addition occurs with the formal cyanide transfer. In this mechanism, SiCN can coordinate to Rh(tmp) in a linear, kinetically indistinguishable N- or C-bound form. The C-bound (i.e., isonitrile) form may be the more preferred coordination mode, as Me_3SiNC is also present in Me_3SiCN in small amounts and the proportion increases at elevated temperature,[28,29] and the sluggish reaction of ^tBuCN with Rh(tmp) at 70 °C supports the C-bound (isonitrile) form of Me_3SiCN in coordination (Scheme 1). Also, the preferred coordination of the isonitrile form in Me_3SiCN with transition metal complexes has been documented.[30] Hertler and co-workers have reported that tri(*tert*-butoxy)silyl cyanide and -isocyanide

(24) Halpern, J. *Acc. Chem. Res.* **1970**, *3*, 386−392.

(25) (a) Collman, J. P.; Boulatov, R. *J. Am. Chem. Soc.* **2000**, *122*, 11812−11821. (b) Marzilli, L. G.; Marzilli, P. A.; Halpern, J. *J. Am. Chem. Soc.* **1970**, *92*, 5752−5753.

(26) Mak, K. W.; Chan, K. S. *J. Am. Chem. Soc.* **1998**, *120*, 9686−9687.

(27) (a) Pestovsky, O.; Bakac, A. *Inorg. Chem.* **2002**, *41*, 3975−3982. (b) Acharyya, R.; Dutta, S.; Basuli, F.; Peng, S.-M.; Lee, G.-H.; Falvello, L. R.; Bhattacharya, S. *Inorg. Chem.* **2006**, *45*, 1252−1259. (c) Osakada, K.; Koizumi, T.-a.; Yamamoto, T. *Bull. Chem. Soc. Jpn.* **1997**, *70*, 189−195. (d) Wang, Z.-Q.; Turner, M. L.; Taylor, B. F.; Maitlis, P. M. *Polyhedron* **1995**, *14*, 2767−2769.

(28) Bither, T. A.; Knoth, W. H.; Lindsey, R. V., Jr.; Sharkey, W. H. *J. Am. Chem. Soc.* **1958**, *80*, 4150−4153.

(29) Rüchardt, C.; Meier, M.; Haaf, K.; Pakusch, J.; Wolber E. K. A.; Müller, B. *Angew. Chem.* **1991**, *30*, 893−1050.

(30) Seyferth, D.; Kahlen, N. *J. Am. Chem. Soc.* **1960**, *82*, 1080−1082.

Table 3. Rate Constants of Reaction 3

entry	temp (°C)	[Rh(tmp)] $\times 10^5$ (M)	[Me_3SiCN] $\times 10^2$ (M)	[py] $\times 10^3$ (M)	[pyRh(tmp)CN] $\times 10^5$ (M)	$k'_{obs} \times 10^4$ (s^{-1})	$k_{obs} \times 10^2$ ($M^{-1}\,s^{-1}$)
1	60.0	9.93	1.29	4.97		4.64 ± 0.14	3.60 ± 0.11
2	70.0	9.60	1.28	4.80		7.00 ± 0.15	5.47 ± 0.12
3		3.28	1.27	4.80		7.37 ± 0.16	5.80 ± 0.13
4		3.28	1.27	4.77	9.60	7.68 ± 0.17	6.05 ± 0.13
5		3.28	1.27	4.79	32.80	7.57 ± 0.16	5.96 ± 0.13
6	80.0	9.60	1.23	9.56		11.60 ± 0.24	9.43 ± 0.19
7	90.0	9.47	1.23	9.46		24.70 ± 0.60	20.08 ± 0.49

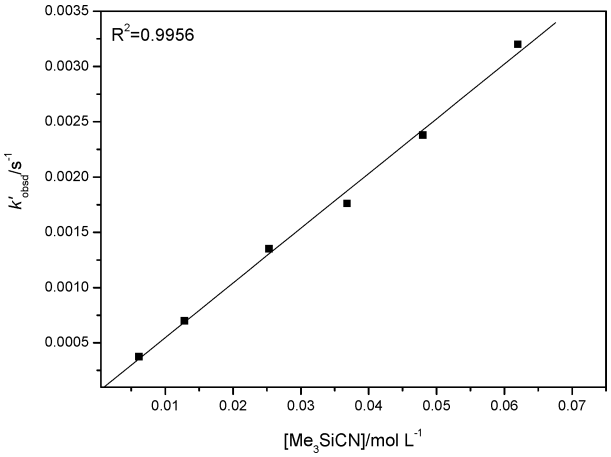

Figure 6. Linear plot of k'_{obs} with [Me_3SiCN] for reaction 3.

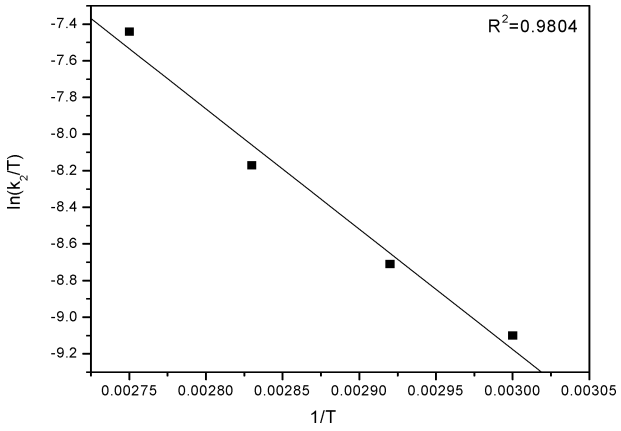

Figure 7. Eyring plot of reaction 16.

$$\text{Rate} = k_2[\text{Rh(tmp)}]_0[\text{Me}_3\text{SiCN}] \qquad (16)$$

$$[\text{Rh(tmp)}]_0 = [\text{Rh(tmp)}]_{\text{total}}$$

equilibrated at room temperature very slowly.[31] The equilibration of cyanide and isocyanide forms in ^{t}BuMe$_2$SiCN may also exist. A Si−NC bond activation occurred, and this cyanide group transfer mechanism occurs in a manner analogous to the halogen abstraction reactions of Co(II) and Cr(II) with organic halides, with the generation of an alkyl radical intermediate and the formation of the more highly stabilized six-coordinate cobalt(III) derivative.[32−34] Likewise, the formation of a six-coordinate pyRh(tmp)CN is very favorable. The other co-intermediate is the free Me_3Si radical. The mechanism is consistent with activation parameters $\Delta H_2^{\ddagger} = 13.1 \pm 1.3$ kcal mol^{-1} and $\Delta S_2^{\ddagger} = -26.3 \pm 3.7$ cal mol^{-1} K^{-1}, typical of a bimolecular atom transfer reaction in cobalt(II) chemistry.[24,35]

To further explore the generality of the proposed cyanide transfer, the reported reactions of Rh(tmp) with alkyl isonitriles by Wayland[5] were reexamined in more detail.

Reactions of BuNC. An immediate color change occurred upon addition of BuNC to a benzene solution of Rh(tmp) at room temperature (eq 18). The reaction was completed within half an hour to result in cleavage of the C−NC bond and quantitative formation of equal amounts of Rh(tmp)Bu(BuNC) and Rh(tmp)CN(BuNC). Rh(tmp)Bu(BuNC) was unstable toward column chromatography and was therefore quantified as Rh(tmp)Bu (Table 4, entry 1). In solution, Rh(tmp)Bu was observed to coordinate with a molecule of BuNC. Table 5 shows that the chemical shifts of the butyl groups were upfield shifted with increasing equivalents of BuNC ligand added and therefore supported BuNC coordination.

$$\text{Rh(tmp)} + \text{RNC} \xrightarrow[\substack{\text{rt}\\ C_6H_6,\ N_2}]{\text{ligand (L)}} \text{Rh(tmp)R} + \text{LRh(tmp)CN} + \text{Rh(tmp)CN(CNR)} \qquad (20)$$

When pyridine was added, both reaction rates and yields decreased significantly. In this case, pyRh(tmp)CN was produced instead of Rh(tmp)CN(BuNC), probably due to the stronger coordination of pyridine (Table 4, entry 2). Likely, coordination with pyridine competed with BuNC and hindered the rhodium center from accessing RNC; therefore, sluggish C−NC bond cleavage resulted. Triphenylphosphine was also not an effective promoter of rate and yield (Table 4, entry 3).

Reactions of ^{t}BuNC with Rh(tmp). When ^{t}BuNC was reacted with Rh(tmp), Rh(tmp)CN(^{t}BuNC) was formed in 57% yield. No alkyl derivative was observed presumably due to the steric hindrance of the *tert*-butyl group in forming Rh(tmp)^{t}Bu in a manner similar to the reaction of ^{t}BuMe$_2$SiCN. Rh(tmp)^{t}Bu is likely very unstable. Indeed, the synthesis of an analogous, sterically hindered (DMG)$_2$Rh^{t}Bu (DMG = dimethylglyoximato) was not successful due to its thermal lability.[36] Similar to the case of BuNC, pyridine slowed the reaction rate and lowered the product yields (Table 4, entries 4−6).

Reactions of Me_3SiCH_2NC with Rh(tmp). The reactions between Me_3SiCH_2NC and Rh(tmp) also proceeded fast at room temperature. However, Rh(tmp)Me was unexpectedly formed in 19% yield. Rh(tmp)CN with and without a coordinated Me_3SiCH_2NC ligand were both produced (Table 4, entries 7−9). No Rh(tmp)CH_2SiMe_3 was observed. Presumably the Me_3SiCH_2 radical is too bulky to react. Alternatively, C−Si bond activation proceeded to yield 12% of Rh(tmp)CH_3.

(31) Hertler, W. R.; Dixon, D. A.; Matthews, E. W.; Davidson, F.; Kitson, F. G. *J. Am. Chem. Soc.* **1987**, *109*, 6532−6533.
(32) Schneider, P. W.; Phelan, P. F.; Halpern, J. *J. Am. Chem. Soc.* **1969**, *91*, 77−81.
(33) Castro, C. E.; Kray, W. C., Jr. *J. Am. Chem. Soc.* **1963**, *85*, 2768−2773.
(34) Halpern, J.; Maher, J. P. *J. Am. Chem. Soc.* **1965**, *87*, 5361−5366.
(35) Halpern, J.; Phelan, P. F. *J. Am. Chem. Soc.* **1972**, *94*, 1881−1886.
(36) (a) Anderson, J. E.; Yao, C.; Kadish, K. M. *J. Am. Chem. Soc.* **1987**, *109*, 1106−1111. (b) Giese, B.; Hartung, J.; Kesselheim, C.; Lindner, H. J.; Svoboda, I. *Chem. Ber.* **1993**, *126*, 1193−1200.

Scheme 1. Transition State of the Reaction of Rh(tmp) with Silyl Isonitriles

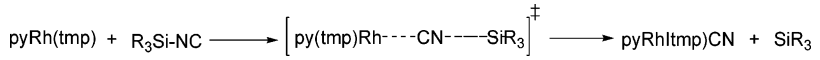

Table 4. Reactions of RNC with Rh(tmp)

entry	substrate[a]	ligand (L)	time/h	product (% yield)[e]		
1	BuNC	none	0.5	Rh(tmp)Bu (45)[f]		Rh(tmp)CN(CNBu) (47)
2	BuNC	py[b]	3	Rh(tmp)Bu (6)[f]	pyRh(tmp)CN (17)	
3	BuNC	Ph_3P[d]	0.5	Rh(tmp)Bu (31)[f]		Rh(tmp)CN(CNBu) (33)
4	^{t}BuNC	none	0.5			Rh(tmp)CN(CN^{t}Bu) (57)
5	^{t}BuNC	py[b]	1		pyRh(tmp)CN (35)	Rh(tmp)CN(CN^{t}Bu) (trace)
6	^{t}BuNC	Ph_3P[d]	0.5			Rh(tmp)CN(CN^{t}Bu) (37)
7	Me_3SiCH_2NC	none	0.5	Rh(tmp)Me(19)	Rh(tmp)CN (45)	Rh(tmp)CN($CNCH_2SiMe_3$) (21)
8	Me_3SiCH_2NC	py[c]	1	Rh(tmp)Me(12)	pyRh(tmp)CN (30)	Rh(tmp)CN($CNCH_2SiMe_3$) (15)
9	Me_3SiCH_2NC	Ph_3P[d]	0.5	Rh(tmp)Me(23)	Rh(tmp)CN (41)	Rh(tmp)CN($CNCH_2SiMe_3$) (29)

[a] 10 equiv. [b] 25 equiv. [c] 2 equiv. [d] 1 equiv. [e] Isolated yield. [f] In solution as Rh(tmp)Bu(BuNC).

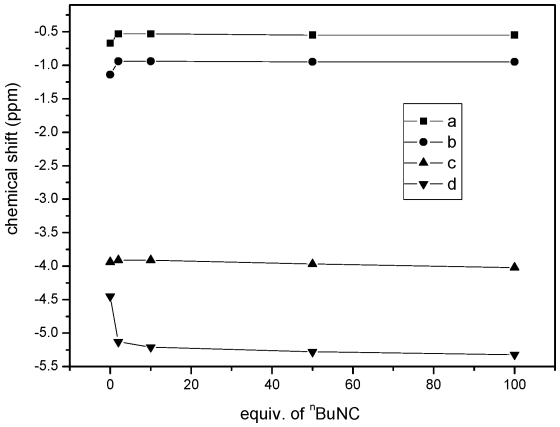

Figure 8. Relation between chemical shift of Rh(tmp)Bu and equivalents of BuNC.

Table 5. ^{1}HNMR Chemical Shifts of the Reaction of Rh(tmp)Bu and BuNC

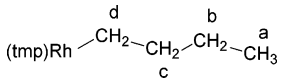

		chemical shift (ppm)			
entry	equiv of BuNC	a	b	c	d
1	0	−0.67	−1.14	−3.94	−4.45
2	2	−0.53	−0.94	−3.91	−5.13
3	10	−0.53	−0.94	−3.91	−5.21
4	50	−0.55	−0.95	−3.97	−5.28
5	100	−0.55	−0.95	−4.02	−5.32

Mechanistic Studies of Rh(tmp) and BuNC in Benzene. A facile, clean, and high-yielding reaction occurred with Rh(tmp) and BuNC. To elucidate the mechanism, kinetic measurements of reaction 20 were therefore performed spectrophotometrically by monitoring the absorbance changes accompanying the reaction at 522 nm at 25.0 °C, with initial concentrations of $(1.11-0.56) \times 10^{-4}$ M for Rh(tmp) and $(0.18-2.15) \times 10^{-2}$ M for BuNC for at least 4 half-lives. Kinetic measurements yielded the rate law shown in eq 22. Pseudo-second-order rate constants k_{obs}', determined from the slopes of second-order rate plots (Figure 9), were plotted against $[BuNC]^2$ to yield the linear plot (Figure 10). The proposed mechanistic scheme depicted in eqs 23−25 conforms to the rate law (eq 22). Incorporating the binding constant (K_1), the rate law was derived as eq 26.

$$2\text{Rh(tmp)} + 3\text{BuNC} \xrightarrow{C_6H_6,\ N_2} \text{Rh(tmp)Bu(BuNC)} + \text{Rh(tmp)CN(BuNC)} \quad (21)$$

$$\text{Rate} = k_{obsd}\,[\text{Rh(tmp)}]^2[\text{BuNC}]^2 \quad (22)$$

Proposed mechanism:

$$\text{Rh(tmp)} + \text{BuNC} \underset{k_{-1}'}{\overset{k_1'}{\rightleftharpoons}} \text{Rh(tmp)(BuNC)} \quad (23)$$

$$\text{Rh(tmp)\,(BuNC)} + \text{Rh(tmp)(BuNC)} \xrightarrow{k_2'(\text{rds})} \text{Rh(tmp)Bu(BuNC)} + \text{Rh(tmp)CN} \quad (24)$$

$$\text{Rh(tmp)CN} + \text{BuNC} \underset{}{\overset{k_3'}{\rightleftharpoons}} \text{Rh(tmp)CN(BuNC)} \quad (25)$$

$$\begin{aligned}\text{Rate} &= \text{d[Rh(tmp)]}/2\text{d}t = -\text{d[Rh(tmp)Bu(BuNC)]}/\text{d}t \\ &= k_2'[\text{Rh(tmp)(BuNC)}]^2 \\ &= k_2'K_1'[\text{Rh(tmp)}]^2[\text{BuNC}]^2\end{aligned} \quad (26)$$

where $K_1' = k_1'/k_{-1}'$

The proposed mechanism consists of a fast precoordination of Rh(tmp) with BuNC.[37,38] Subsequently, the rate-determining step involves the C−NC bond cleavage assisted by a second molecule of Rh(tmp)CNBu in the transition state to simultaneously form Rh−Bu and Rh−CN bonds. Finally, BuNC ligand coordination between the cyanide complex gives Rh(tmp)CN(CNBu). The transition state involves four molecules, two in Rh(tmp) and two in BuNC, fully consistent with the observed rate law.A possible alternative mechanism that merits consideration is that involving ligand-induced disproportionation of the Rh(tmp) complex according to eq 27, followed by nucleophilic attack of the anionic rhodium(I) fragment at the carbon atom of the alkyl group of isonitrile.[31] The latter mechanism seems unlikely in the cleavage of the alkyl−NC bond by the rhodium(II) porphyrin radical for the following reason. Isonitrile ligands are electronically related to carbon monoxide and their coordination chemistry is closely related and well-known.[5] π-Acidic ligands, such as CO or RNC, have much lower affinity

(37) Wayland, B. B.; Sherry, A. E.; Poszmik, G.: Bunn, A. G. *J. Am. Chem. Soc.* **1992**, *114*, 1673−1681.
(38) Paonessa, R. S.; Thomas, N. C.; Halpern, J. *J. Am. Chem. Soc.* **1985**, *107*, 4333−4335.

Scheme 2. Transition State of the Reaction of Rh(tmp) with BuNC

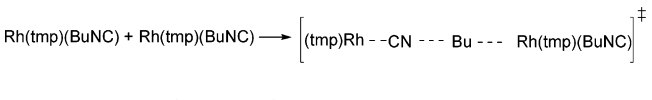

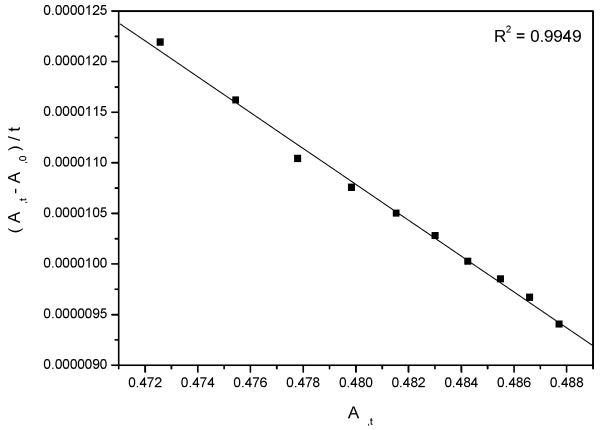

Figure 9. Representative pseudo-second-order rate plots for reaction 20.

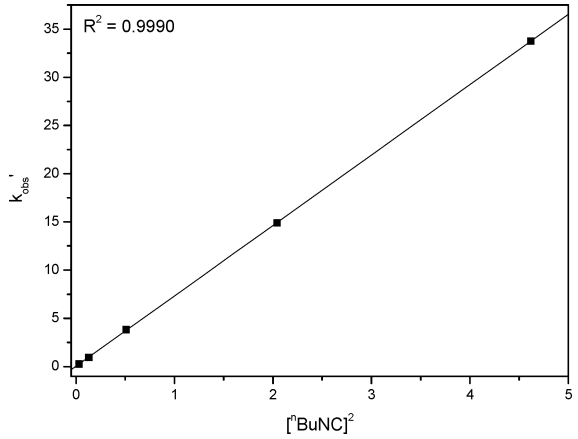

Figure 10. Representative plots of k'_{obsd} vs $[BuNC]^2$ for reaction 20.

to Rh^{III} than Rh^{II} and stabilize the +2 state, and thus suppress disproportionation.[25a] Therefore, disproportionation is less likely for reactions with alkyl isonitriles.

$$2Rh(tmp)CNR \rightleftharpoons Rh(tmp)CNR^{+} + Rh(tmp)CNR^{-} \quad (27)$$

Comparison of Mechanisms of Si−CN and C−NC Activations. The unique mechanisms of the activations of the Si−CN bond in Me_3SiCN or Me_3SiNC and the C−NC bond in BuNC deserve some comments. The activations of Si−CN and C−NC all require precoordination.

1. Coordination Mode. The coordination of both the isocyanide and cyanide form in Me_3SiCN is possible.[19] The C-bound form is productive for the cyanide transfer, while the N-bound form is not. For BuNC, only the C-bound form is possible.

2. Ligand Effect. The rates and yields of products were increased by the addition of pyridine or Ph_3P for the reaction with Me_3SiCN but were suppressed for the reaction with BuNC. For Me_3SiCN, since the activation of the Si−CN bond by two Rh(tmp) is unlikely to occur by backside attack due to the steric hindrance of the Me_3Si group, an alternate mode of cleavage of the Si−NC bond is required and took place at a high temperature of 70 °C. Furthermore, the more electron-rich pyRh(tmp) is formed in order to facilitate oxidative addition. For BuNC, backside attack by Rh(tmp) is possible for the stercially less hindered primary Bu group, and the reaction occurred even at room temperature with the assistance of two Rh(tmp) molecules. As the σ-donating series of ligands follow the order py > RCN > Ph_3P > RNC,[39] addition of pyridine or Ph_3P would displace the weaker BuNC from Rh(tmp)BuNC and decrease either the rates or the yields of reactions, presumably partially by disproportionation of Rh(tmp)L (L = py or Ph_3P).[9−12]

Conclusion

In summary, we have discovered the novel bond activation of silylnitriles by rhodium(II) porphyrin. The reactions were promoted by pyridine and Ph_3P. The mechanism of oxidative addition Si−CN bond activation of Me_3SiCN has been identified to be a bimolecular reaction with the cyanide group transfer to rhodium being the rate-controlling step. The C−NC bonds of alkyl isonitriles have been successfully activated by Rh(tmp). Pyridine and Ph_3P inhibited the bond activation. The rate law of reaction of BuNC with Rh(tmp) was second-order in both Rh(tmp) and BuNC. The cleavage of C−NC of coordinated BuNC was assisted by two Rh(tmp).

Experimental Section

General Procedures. All materials were obtained from commercial suppliers and used without further purification unless otherwise specified. Benzene was distilled from sodium. Hexane was freshly distilled from calcium chloride. Benzene-d_6 was vacuum distilled from sodium, degassed three times by the freeze−thaw−pump method, and stored in a Teflon screwhead stoppered flask. Pyridine was distilled over KOH under N_2. Triphenylphosphine was recrystallized from EtOH. Chromatographic purification of products was carried out in air using silica gel. Samples for elemental analysis were prepared by vacuum-drying (0.005 mmHg) at 50−60 °C for 2 days.

Reaction of Rh(tmp) and Me_3SiCN with Pyridine Added. To a Teflon screwhead stoppered flask containing Rh(tmp) (0.0088 mmol) dissolved in C_6H_6 (4.0 mL) under nitrogen at rt, prepared from the photolysis of Rh(tmp)Me (10.0 mg) in C_6H_6 (4.0 mL) in 80% yield,[13] were added distilled pyridine (2.0 μL, 0.02 mmol) and degassed trimethylsilylnitrile (0.01 mL, 0.08 mmol), respectively. The resultant reaction mixture was heated at 110 °C for 1 h under nitrogen in the absence of light. Rh(tmp) was completely consumed, as no Rh(tmp)CH_2Cl formed from the reaction of residual Rh(tmp) with CH_2Cl_2 by TLC analysis. The crude product was purified by chromatography on silica gel eluting with a solvent mixture of hexane/CH_2Cl_2 (10:1) to hexane/CH_2Cl_2 (5:1) to give an orange solid of Rh(tmp)$SiMe_3$ (3.8 mg, 4.0 μmol, 88%), R_f = 0.55 (hexane/CH_2Cl_2, 5:1); ^1H NMR (C_6D_6, 300 Hz) δ −3.07 (s, 9 H), 1.63 (s, 12 H), 2.41 (s, 24 H), 6.84 (s, 4 H), 7.41 (s, 4 H) 8.69 (s, 8 H); ^1H NMR ($CDCl_3$, 300 Hz) δ −3.47 (s, 9 H), 1.52 (s, 12 H), 2.52 (s, 12 H), 2.60 (s, 12 H), 7.17 (s, 4 H), 7.30 (s, 4 H), 8.43 (s, 8 H); ^{13}C NMR (C_6D_6, 75.5 Hz) δ 1.4, 21.4, 21.5, 23.0, 30.2, 127.1, 131.0, 137.7, 138.5, 140.1, 143.5; ^{13}C NMR ($CDCl_3$, 75.5 Hz) δ 1.0, 21.3, 21.4, 22.7, 29.7, 127.8, 130.4, 138.3, 138.4, 142.9; HRMS (FABMS) calcd for $(C_{59}H_{61}N_4SiRh)^+$ *m/z* 956.3715, found *m/z* 956.3729. Anal. Calcd for $C_{59}H_{61}N_4SiRh$: C, 74.04; H, 6.42; N, 5.85. Found: C, 74.18; H, 6.61; N, 5.64. A deep red solid

(39) Huheey, J. E. *Inorganic Chemistry*, 2nd ed.; Harper & Row: New York, 1978; p 460.

of pyRh(tmp)CN (2.8 mg, 2.8 μmol, 81%) was also obtained. R_f = 0.30 (100% CH_2Cl_2); ^{1}H NMR ($CDCl_3$, 300 MHz) δ 1.26 (d, 2 H, J = 6.0 Hz), 1.59 (s, 12 H), 1.95 (s, 12 H), 2.60 (s, 12 H), 4.97 (t, 2 H, J = 6.9 Hz), 6.00 (t, 1 H, J = 7.8 Hz), 7.19 (s, 4 H), 7.28 (s, 4 H), 8.60 (s, 8 H); ^{13}C NMR ($CDCl_3$, 75 MHz) 21.36, 21.60, 22.08, 29.85, 118.47, 127.43, 128.09, 131.46, 134.86, 138.47, 140.26, 141.75, 146.22, 158.80; HRMS (FABMS) calcd for $(C_{62}H_{57}N_6Rh)^+$ m/z 989.3773, found m/z 989.3771; IR (KBr, cm^{-1}) ν 2305, 2365. The single crystal was grown from THF.

Reaction of Rh(tmp) and ^{t}BuMe$_2$SiCN with Pyridine Added. Distilled and degassed pyridine (2 μL, 0.02 mmol) was added to a solution of Rh(tmp) (0.0088 mmol) at rt. Then degassed *tert*-butyldimethylsilylnitrile (0.10 mL, 0.08 mmol, 0.88M in benzene) was added to the above solution and then heated at 110 °C for 1 day under N_2 in the absence of light. The crude product was purified by chromatography on silica gel eluting with a solvent mixture of hexane/CH_2Cl_2 (10:1) to hexane/CH_2Cl_2 (5:1) to give an orange solid of Rh(tmp)Si^{t}BuMe$_2$ (0.8 mg, 0.8 μmol, 18%), R_f = 0.64 (hexane/CH_2Cl_2, 5:1); ^{1}H NMR (C_6D_6, 300 MHz) δ −2.88 (s, 6 H), −1.25 (s, 9 H), 1.91 (s, 12 H), 2.41 (s, 12 H), 2.56 (s, 12 H), 6.91 (s, 4 H), 7.42 (s, 4 H), 8.66 (s, 8 H); HRMS (FABMS) calcd for $(C_{62}H_{67}N_4SiRh)^+$ m/z 998.4185, found m/z 998.4179. A deep red solid of pyRh(tmp)CN (3.7 mg, 3.7 μmol, 85%), R_f = 0.30 (CH_2Cl_2), was also obtained.

Reaction of Rh(tmp) and Me$_3$SiCN with PPh$_3$ Added. A triphenylphosphine solution (0.1 mL, 0.01 mmol) was added to a solution of [Rh(tmp)] at rt. Degassed trimethylsilylcyanide (0.01 mL, 0.08 mmol) was added to the above solution. After heating at 110 °C for 3 h under N_2 in the absence of light, the crude product was purified by chromatography on silica gel eluting with hexane/CH_2Cl_2 (10:1) to hexane/CH_2Cl_2 (5:1) to give an orange solid of Rh(tmp)SiMe$_3$ (3.3 mg, 3.5 μmol, 79%) with R_f = 0.55 (hexane/CH_2Cl_2, 5:1) as well as a red solid, Rh(tmp)CN (3.1 mg, 3.4 μmol, 78%): ^{1}H NMR (C_6D_6, 300 MHz) δ 1.92 (s, 12 H), 1.98 (s, 12 H), 2.42 (s, 12 H), 8.87 (s, 8 H).

Reaction of Rh(tmp) and ^{t}BuMe$_2$SiCN with PPh$_3$ Added. A triphenylphosphine solution (0.1 mL, 0.01 mmol) was added to a solution of [Rh(tmp)] at rt. Degassed *tert*-butyldimethylsilyl cyanide (0.10 mL, 0.08 mmol, 0.88 M in benzene) was added, and the solution was heated at 110 °C for 1 day under N_2 in the absence of light. The crude product was purified by chromatography on silica gel to give an orange solid of Rh(tmp)Si^{t}BuMe$_2$ (0.2 mg, 0.2 μmol, 2%).

Reaction of Rh(tmp) and ^{t}BuNC. ^{t}BuNC (0.01 mL, 0.08 mmol), which was degassed by the freeze−pump−thaw method (3 cycles), was added via a microsyringe to a benzene solution of Rh(tmp) (0.0088 mmol), and the reaction mixture was stirred at rt for 0.5 h under N_2 in the absence of light. The crude product was purified by chromatography on silica gel using a solvent mixture of CH_2Cl_2 as the gradient eluent. A deep red solid of Rh(tmp)CN(CN^{t}Bu) (5.0 mg, 5.0 μmol, 57%) was obtained, R_f = 0.27 (100% CH_2Cl_2); ^{1}H NMR (C_6D_6, 300 MHz) δ −0.99 (s, 9 H), 1.94 (s, 24 H), 2.44 (s, 12 H), 7.07 (s, 4 H), 7.19 (s, 4 H), 8.89 (s, 8 H); ^{13}C NMR ($CDCl_3$, 75 MHz) δ 21.99, 22.17, 22.78, 28.77, 118.86, 127.89, 128.64, 131.71, 138.18, 138.96, 139.28, 140.60, 142.44; HRMS-(FABMS) calcd for $(C_{62}H_{61}N_6Rh)^+$ m/z 992.4007, found m/z 992.4037. Anal. Calcd for $C_{62}H_{61}N_6Rh$: C, 74.98; H, 6.19; N, 8.46. Found: C, 74.59; H, 6.13; N, 8.06.

Reaction of Rh(tmp) and ^{t}BuNC with Pyridine Added. Distilled and degassed pyridine (2 μL, 0.02 mmol) was added to a solution of Rh(tmp) (0.0088 mmol) at rt. Then degassed ^{t}BuNC (0.01 mL, 0.08 mmol) was added to the above solution, and the mixture was then stirred at rt for 1 h under N_2 in the absence of light. The crude product was purified by chromatography on silica gel eluting with a solvent mixture of hexane/CH_2Cl_2 (10:1) to hexane/CH_2Cl_2 (5:1) to give red deep solids of pyRh(tmp)CN (1.2 mg, 1.2 μmol, 35%).

Reaction of Rh(tmp) and BuNC.[5] BuNC (0.01 mL, 0.08 mmol), which was degassed by the freeze−pump−thaw method (3 cycles), was added via a microsyringe to a benzene solution of Rh(tmp) (0.0088 mmol), and the reaction mixture was stirred at rt for 0.5 h under N_2 in the absence of light. The crude product was purified by chromatography on silica gel using a solvent mixture of hexane/CH_2Cl_2 (10:1) to hexane/CH_2Cl_2 (5:1) as the gradient eluent. An orange solid of Rh(tmp)Bu (3.7 mg, 3.9 μmol, 45%) was obtained, R_f = 0.61 (hexane/CH_2Cl_2, 5:1); ^{1}H NMR (C_6D_6, 300 MHz) δ −4.45 (td, 2 H, $^2J_{Rh-H}$ = 3 Hz, J = 7.5 Hz), −3.94 to −3.83 (m, 2 H), −1.14 to −1.04 (m, 2 H), −0.67 (t, 3 H, J = 7.5 Hz), 1.91 (s, 12 H), 2.18 (s, 12 H), 2.44 (s, 12 H), 7.12 (s, 4 H), 7.29 (s, 4 H), 8.75 (s, 8 H); HRMS (FABMS) calcd for $(C_{60}H_{61}N_4Rh)^+$ m/z 940.3946, found m/z 940.3971. A deep red solid of Rh(tmp)CN-(CNBu) (4.1 mg, 4.1 μmol, 47%) was obtained, R_f = 0.55 (hexane/CH_2Cl_2, 5:1); ^{1}H NMR (C_6D_6, 300 MHz) δ −0.93 to −0.92 (m 4 H), −0.29 (t, 3 H, J = 6.9 Hz), 0.15 (t, 2 H, J = 6 Hz), 1.82 (s, 12 H), 2.05 (s, 12 H), 2.44 (s, 12 H), 7.04 (s, 4 H), 7.21 (s, 4 H), 8.91 (s, 8 H); HRMS (FABMS) calcd for $(C_{62}H_{61}N_6Rh)^+$ m/z 993.4086, found m/z 993.4066.

Reaction of Rh(tmp) and BuNC with Pyridine Added. Distilled and degassed pyridine (2 μL, 0.02 mmol) was added to a solution of Rh(tmp) (0.0088 mmol) at rt. Then degassed BuNC (0.01 mL, 0.08 mmol) was added to the above solution, and the mixture was then stirred at rt for 3 h under N_2 in the absence of light. The crude product was purified by chromatography on silica gel eluting with a solvent mixture of hexane/CH_2Cl_2 (10:1) to hexane/CH_2Cl_2 (5:1) to give an orange solid of Rh(tmp)Bu (0.5 mg, 0.5 μmol, 6%); red deep solids of pyRh(tmp)CN (1.5 mg, 1.5 μmol, 17%) were also obtained.

Reaction of Rh(tmp) and Me$_3$SiCH$_2$NC with Pyridine Added. Distilled and degassed pyridine (2 μL, 0.02 mmol) was added to a solution of Rh(tmp) (0.0088 mmol) at rt. Then degassed Me$_3$SiCH$_2$-NC (0.01 mL, 0.08 mmol) was added to the above solution, and the mixture was then stirred at rt for 1 h under N_2 in the absence of light. The crude product was purified by chromatography on silica gel eluting with a solvent mixture of hexane/CH_2Cl_2 (10:1) to hexane/CH_2Cl_2 (5:1) to give an orange solid of Rh(tmp)Me (1.0 mg, 1.1 μmol, 12%) with R_f = 0.57 (hexane/CH_2Cl_2, 5:1); ^{1}H NMR (C_6D_6, 300 MHz) δ −5.26 (d, 3 H $^2J_{RhH}$ = 2.7 Hz), 1.72 (s, 12 H), 2.25 (s, 12 H), 2.43(s, 12 H), 7.07 (s, 4 H), 7.20 (s, 4 H), 8.75 (s, 8 H); a red deep solid of pyRh(tmp)CN (2.6 mg, 2.6 μmol, 30%) was also obtained and deep red solids of Rh(tmp)CN(CNCH$_2$SiMe$_3$) (2.8 mg, 2.8 μmol, 15%) with R_f = 0.50 (CH_2Cl_2/EA, 100:3); ^{1}H NMR (C_6D_6, 300 MHz) δ −1.62 (s, 9 H), −0.22 (s, 2 H), 1.36 (s, 12 H), 1.83 (s, 12 H), 2.43 (s, 12 H), 6.89 (s, 4 H), 7.23 (s, 4 H), 8.90 (s, 8 H); ^{13}C NMR ($CDCl_3$, 75 MHz) δ −4.50, 22.16, 22.32, 22.65, 118.86, 127.87, 128.64, 131.76, 138.15, 138.91, 139.00, 140.97, 142.33; HRMS (FABMS) calcd for $(C_{62}H_{63}N_6SiRh)^+$ m/z 1022.3965, found m/z 1002.3933. Anal. Calcd for $C_{62}H_{63}N_6SiRh$: C, 72.78; H, 6.21; N, 8.21. Found: C, 72.46; H, 6.33; N, 8.00.

Kinetic Studies on Reaction of Rh(tmp) and Me$_3$SiCN with Pyridine Added. Kinetic studies were carried out in the temperature range (60−90) ± 0.2 °C maintained by a constant-temperature circulating bath. Rh(tmp)Me (5 mg) was dissolved in benzene (4 mL) in a Rotaflo flask and degassed, and after photolysis a stock solution of Rh(tmp) (2.225×10^{-3} M) was produced. Pyridine (1.95×10^{-1} M), substrate Me$_3$SiCN (1.661 M), and pyRh(tmp)CN (2.225×10^{-3} M) were prepared and degassed. A measured amount of the stock solution of Rh(tmp) and pyridine were added with benzene in a curvette-Schlenck UV cell, and the mixture was thermally equilibrated for 30 min. Then the Me$_3$SiCN solution in benzene was added to the mixture quickly, and absorbance was measured at 538 nm.

UV Titration of Rh(tmp) with Pyridine. The UV titrations were carried out on a UV−vis spectrometer equipped with a temperature controller. The titrations were carried out at temperatures of 20.0,

25.0, 30.0, 35.0, and 40.0 (±0.2) °C. The temperatures of the solutions were measured by a thermocouple wire placed in a UV cell that was placed inside the sample compartment. Benzene was freshly distilled over sodium under N_2, and pyridine was distilled over NaOH under N_2. Stock solutions of Rh(tmp) in benzene (~5.45 × 10^{-6} M) and pyridine in benzene (~1.0 × 10^{-1} M) were prepared. The solutions of Rh(tmp) (3.00 mL) was transferred to a Teflon-stoppered Schlenck UV cell with a gastight syringe under N_2. Pyridine solution was then titrated into the Rh(tmp) solutions via a gastight microsyringe at 2.0 μL steps up to a total of 20.0 μL and then at 4.0 μL steps up to a total of 60.0 μL of pyridine solution added. Finally 100 μL of neat pyridine was added to the sample solution to obtain the estimated absorbance for the Rh(tmp)−pyridine complex. The UV spectra were scanned at 600 nm/min between 350 and 700 nm. The experimental absorbance was measured at 536 nm. The binding constants and the number of pyridine ligands coordinated to each Rh(tmp) complex were calculated by the equation[40]

$$\log K_n = \log\frac{A_e - A_m}{A_n - A_e} - n \log[L]$$

where n = number of pyridine ligands coordinated to each Rh(tmp), K_n = binding constant, [L] = concentration of pyridine in the UV sample, A_e = experimental absorbance measured (volume correction made), A_m = absorbance of the Rh(tmp) without pyridine, A_n = theoretical absorbance obtained for the Rh(tmp)−pyridine complex (obtained from the absorbance measured for the infinite point with volume correction).

The measured (A_e) were corrected for volume change due to the addition of ligand solution and the thermal expansion/contraction by $V_t = V_0(1 + \beta_t)$ and $\beta = 0.00372$ (for benzene).[41]

Kinetic Studies on Reaction of Rh(tmp) and BuNC. Kinetic studies were carried out at the temperature 25.0 ± 0.2 °C maintained by a constant-temperature circulating bath. After photolysis the stock solution of Rh(tmp) (1.11 × 10^{-3} M) was produced. Substrate BuNC (0.535 M) was prepared and degassed. A measured amount of the stock solution of Rh(tmp) was added with benzene in a curvette-Schlenck UV cell and was thermally equilibrated for 30 min. Then the BuNC solution in benzene was added to the mixture quickly, and absorbance was measured at 522 nm.

Acknowledgment. We thank the Research Grants Council of Hong Kong of the SAR of China for financial support (No. 400203).

Supporting Information Available: Kinetic data, NMR spectra, and X-ray structural data (cif). This material is available free of charge via the Internet at http://pubs.acs.org.

OM0605276

(40) Perkampus H. H. *UV−Vis Spectroscopy and Its Applications*; Springer-Verlag: Berlin, 1992.

(41) Atkins. P. *Physical Chemistry*, 6th ed.; Oxford, 1998.